Supporting Information

Amphoteric reactivity of iron(III)-hydroperoxo complex generated by proton- and salicylate-assisted dioxygen activation

Chaewon An,[a] Hyeri Jeon,[a] Yool Lee,[a] Geonwoo Park,[b] Hyun S. Ahn,*[b] Seungwoo Hong*[a]

[a] *Department of Chemistry and Nanoscience, Ewha Womans University, Seoul 03760, Republic of Korea.*

[b] *Department of Chemistry, Yonsei University, Seoul, 03722, Republic of Korea.*

E-mail: ; hsw@ewha.ac.kr; ahnhs@yonsei.ac.kr

Experimental Section

Materials and Instrumentation. Commercially available chemicals were used without further purification unless otherwise indicated. Solvents were dried according to published procedures and distilled under Ar prior to use.[S1] D_2O (98% D-enriched) was purchased from ICON Services Inc. (Summit, NJ, USA). The nonheme iron(II) complex was prepared according to the modified literature methods.[S2] UV-vis spectra were recorded on a Hewlett Packard Agilent Cary 8454 UV-visible spectrophotometer equipped with a T2/sport temperature controlled cuvette holder. X-ray diffraction (XRD) patterns were acquired using D/MAX-2200/VPC Rigaku at the National Research Facilities and Equipment Center (NanoBio·Energy Materials Center) at Ewha Womans University. Electrospray ionization mass spectra (ESI MS) were collected on a Thermo Finnigan (San Jose, CA, USA) LTQ^{TM} XL ion trap instrument, by infusing samples directly into the source at 5.0 μL/min using a syringe pump. The spray voltage was set at 4.7 kV and the capillary temperature at 120 ºC. X-band EPR spectra were recorded at 80 K using an X-band Bruker EMX-plus spectrometer equipped with a dual mode cavity (ER 4116DM) and a JEOL X band spectrometer (JESFA100). Electrochemical measurements were performed on a CHI617B electrochemical analyzer (CH Instruments, Inc.) in CH_3CN containing 0.10 M Bu_4NPF_6 ($TBAPF_6$) or in H_2O containing 0.10 M $NaClO_4$ as supporting electrolytes at 20 °C, respectively. A conventional three-electrode cell was used with a glassy carbon working electrode (surface area of 0.030 cm^2), a platinum wire as a counter electrode and an Ag/Ag^+ electrode as a reference electrode (in CH_3CN) or an Ag/AgCl, 1.0 M KCl electrode as a reference electrode (in H_2O), respectively. The glassy carbon working electrode was routinely polished with BAS polishing alumina suspension and rinsed with acetone and acetonitrile before use. The measured potentials were recorded with respect to an Ag/Ag^+ (0.010 M) reference electrode (in CH_3CN) or an Ag/AgCl, 1.0 M KCl reference electrode (in H_2O), respectively. All potentials (vs Ag/Ag^+ or Ag/AgCl) were converted to values vs Fc/Fc^+ by subtracting 0.09 V or 0.02 V, respectively. Solid IR signals for samples were recorded on an IR instrument (Remspec #: 626). Solid IR data of both **2-OOH** (12 mM) and **2-OOD** (12 mM) were obtained by isolating **2** under N_2 atmosphere, respectively.

DFT Calculations. Geometry optimization of **2** was fully optimized by using the Gaussian 09[S3] program with the B3LYP density functional at the LANL2DZ/6-31G** level,[S4-S17]

whereas no imaginary frequencies were observed. In addition, the solvent effect of the polarizable continuum model (PCM) with acetonitrile (ε = 35.688) and temperature (293 K) was also applied.[S18]

Synthesis of N3PPh$_3$ ligand. The cationic N3PPh$_3$ ligand (N3PPh$_3$ = (3-(bis(pyridine-2-ylmethyl)amino)triphenylphosphonium) was synthesized in two steps. A mixture CH_3CN solution of 3-bromopropylamine hydrobromide (10.0 mmol) and triphenylphosphine (10.0 mmol) was stirred at 82 ℃ under reflux for 12 hours. The mixture was cooled down to room temperature. Hexane was added to the solution and the resulting solution was dissolved in isopropyl alcohol. Diethyl ether was then added, and the reaction solution was left overnight in refrigerator to give the product as a white solid (compound 1). The next step is mixing compound **1** (5.00 mmol), 2-pyridinecarboxaldehyde (10.0 mmol), acetic acid (10.0 mmol), and sodium triacetoxyborohydride (13.3 mmol) in THF (30.0 mL). The mixture was stirred at room temperature for 3 days. After removing the solvent in vacuo, the residue was dissolved in CH_2Cl_2 and washed three times with saturated $NaHCO_3$ solution, dried over $NaSO_4$, filtered and evaporated. The N3PPh$_3$ ligand was isolated as yellowish-brown oil (yield ~ 70%). Elemental analysis: calcd. for $C_{33}H_{33}BrN_3P$ (N3PPh$_3$Br): C, 68.04; H, 5.71; N, 7.21.[S2]

Synthesis and Characterization of Mononuclear Iron(II) Complexes. The mononuclear iron(II) complex bearing N3PPh$_3$ ligand, $[Fe^{II}(N3PPh_3)]^{3+}$, was prepared by reacting N3PPh$_3$ ligand and slight excess of $Fe(ClO_4)_2{\cdot}xH_2O$ in CH_3CN (Scheme S1a). $[Fe^{II}(N3PPh3)(SA)]^{2+}$ (**1**, SA = salicylate), was obtained by reacting $[Fe^{II}(N3PPh_3)]^{3+}$ with 1.5 equiv of sodium salicylate in CH_3CN at 20 °C. The iron(III)-hydroperoxo complex, $[Fe^{III}(OOH)(N3PPh_3)(SA)]^{2+}$ (**2**), was synthesized by treating the solution of **1** with 2.0 equiv of perchloric acid in air-saturated CH_3CN at 20 ºC. Isolated **2** was prepared by adding excess diethyl ether to the CH_3CN-solution containing 2.0 mM of **2** under N_2 atmosphere and dried in vacuo. Elemental analysis: calcd (found). for $C_{44}H_{44}Cl_2FeN_5O_{11}P$: C, 47.65 (47.11); H, 4.45 (4.54); N, 7.36 (7.17).

Reactivity Studies. Kinetic measurements were performed on a Hewlett Packard 8453 photodiode-array spectrophotometer for the oxygen atom transfer and O−H bond activation and aldehyde oxidation reactions by **2** in CH_3CN at 20 °C. Reactions were run in a 1.0 cm UV

cuvette, monitoring UV-vis spectral changes of reaction solutions. Rate constants were determined under pseudo-first-order conditions (e.g., [substrate]/[**2**] > 10) by fitting the absorbance changes at 570 nm due to **2**. For the oxygen atom transfer, O−H bond activation and and aldehyde oxidation reactions by **2**, the time dependence of the absorbance at 570 nm due to the decay of **2** was fitted with single exponential function to give k_{obs} (s^{-1}) under the pseudo-first-order conditions in CH_3CN at 20 °C.

The kinetic experiments were run at least in triplicate, and the data reported represent the average of these reactions.

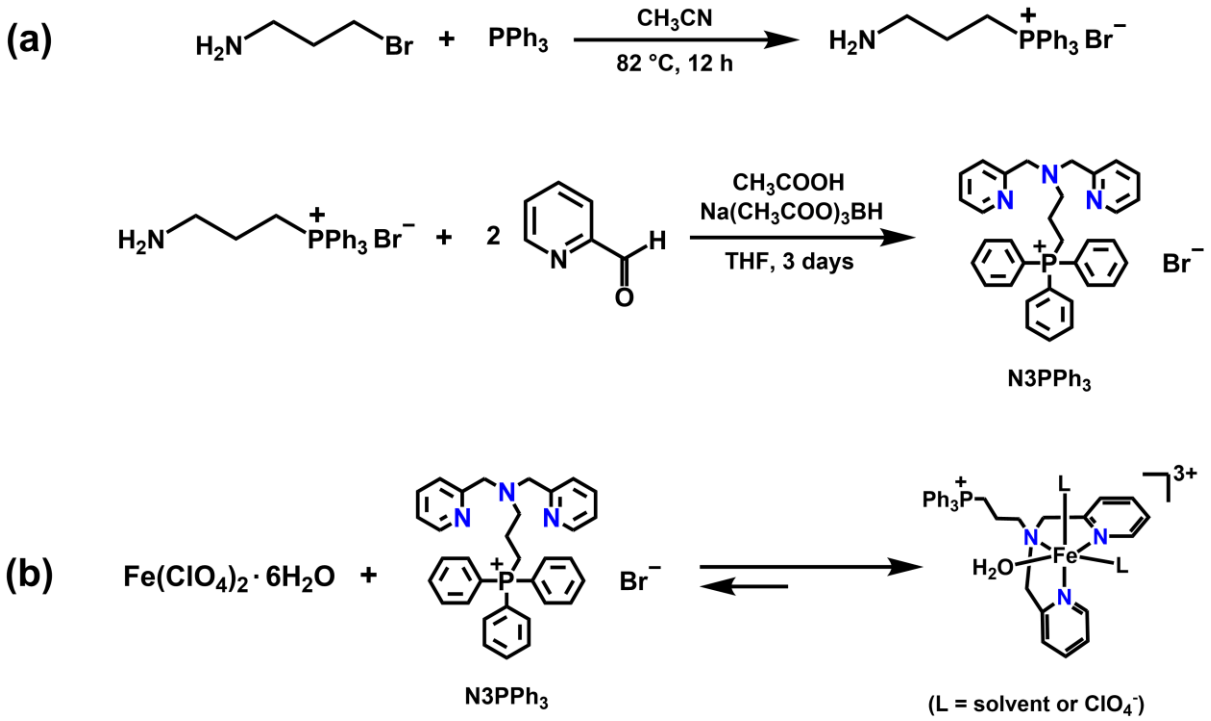

Scheme S1 Synthetic route of (a) $N3PPh_3$ ligand and (b) $[Fe(N3PPh_3)(L)]^{3+}$ (L = solvent or anion)

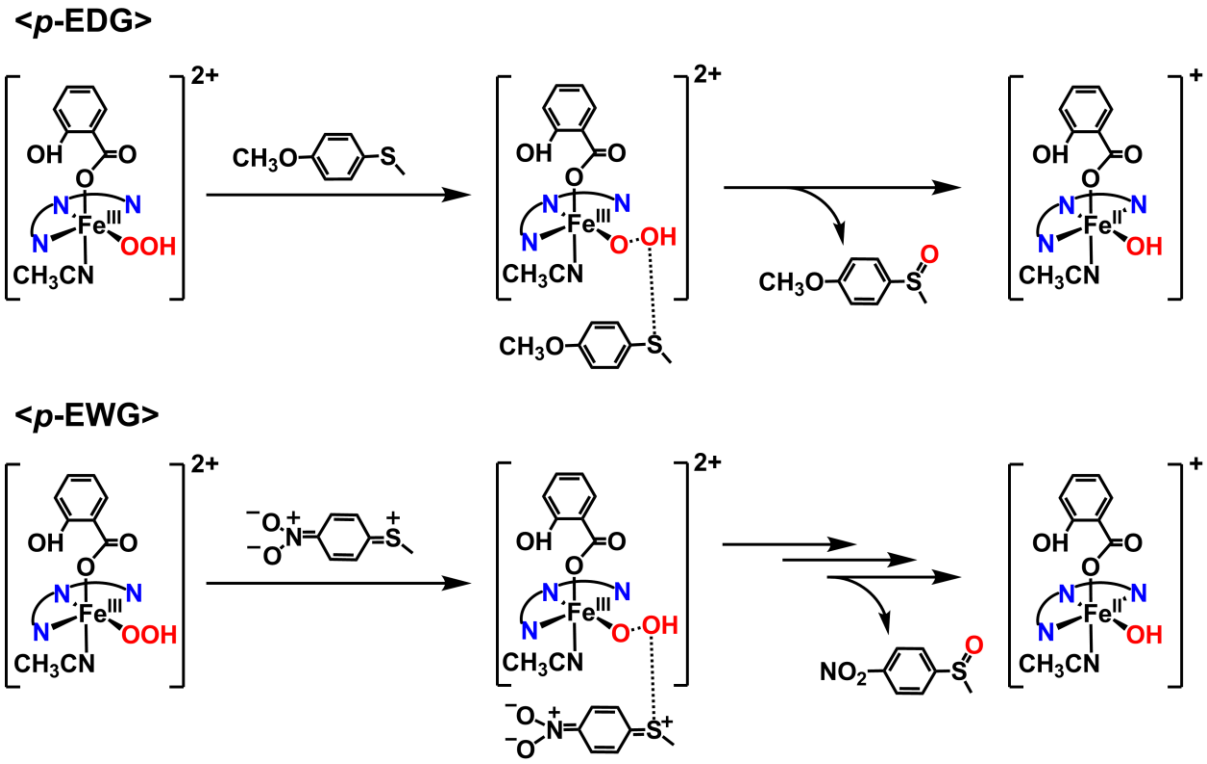

Scheme S2 Proposed mechanisms of oxygen atom transfer reactions by **2**.

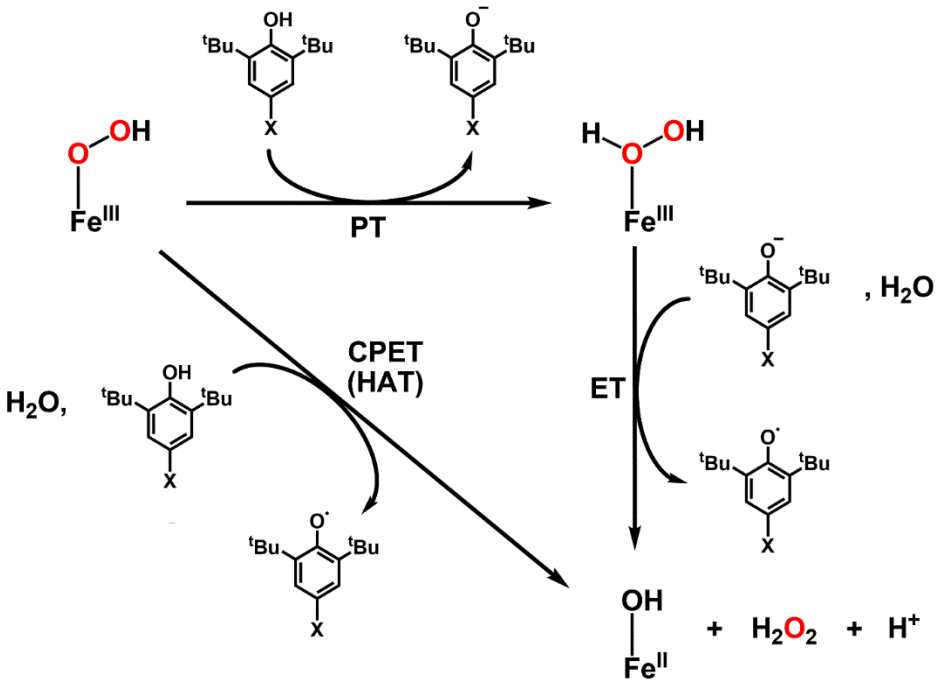

Scheme S3. Proposed mechanisms of O-H bond activation reactions by **2**.

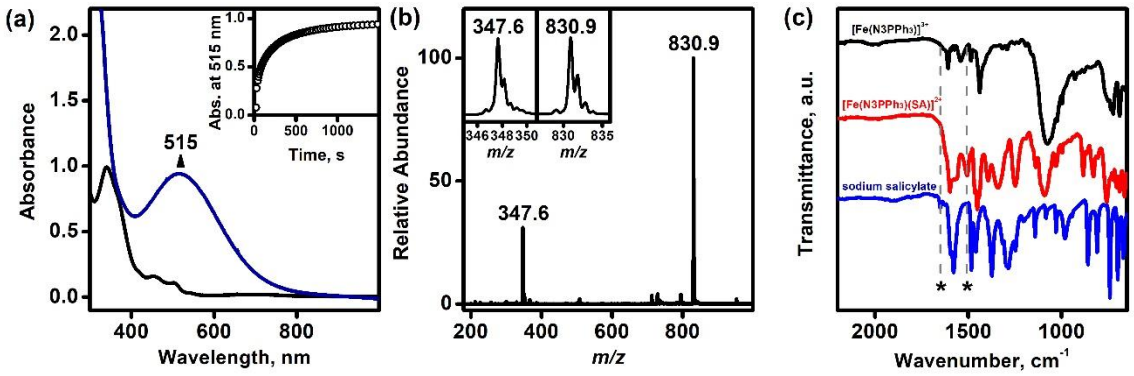

Fig. S1 (a) UV-vis spectral changes obtained in the reaction between **[**$Fe(N3PPh_3)$**]**$^{3+}$ (0.50 mM, black line) and sodium salicylate (1.0 mM, blue line) in CH_3CN at 20 °C. (b) ESI-MS spectrum of **[**$Fe(N3PPh_3)(SA)$**]**$^{2+}$ (**1**). The peaks at *m/z* = 347.6 and 830.9 correspond to $[Fe(N3PPh_3)(SA)]^{2+}$ (calculated *m/z* = 347.6) and $[Fe(N3PPh_3)(SA)(CH_3CN)(CH_3OH)_2(CH_3O)]^{+}$ (calculated *m/z* = 831.3), respectively. (c) Overlaid ATR FT-IR spectra of the $[Fe(N3PPh_3)]^{3+}$ (black line), **[**$Fe(N3PPh_3)(SA)$**]**$^{2+}$ (red line), and sodium salicylate (blue line). The spectra were recorded from solid samples deposited on the ATR crystal.

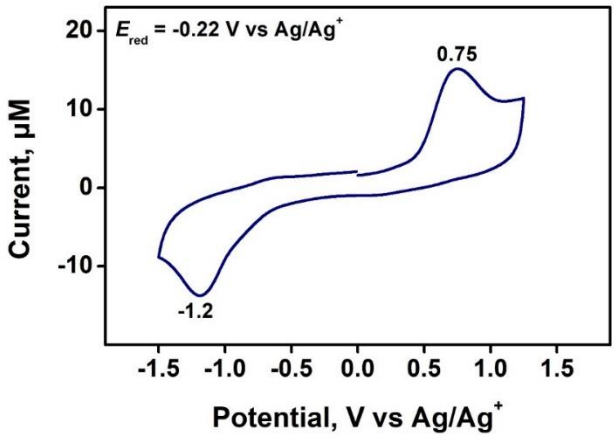

Fig. S2 Cyclic voltammogram of **1** (2.0 mM, blue line) in CH_3CN with a glassy carbon working electrode at 20 °C.

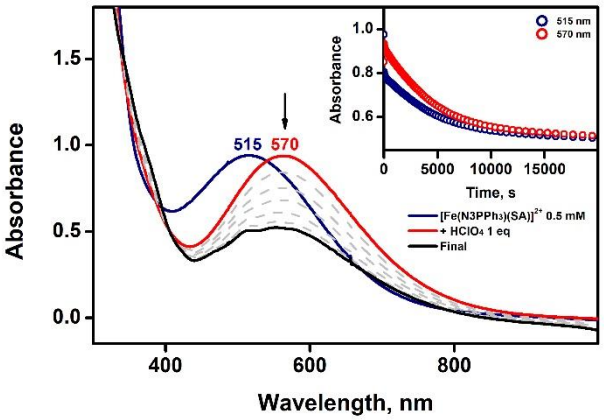

Fig. S3 UV-vis spectral changes of **2** obtained in the reaction of between **1** (0.50 mM, blue line) with perchloric acid (0.50 mM, red line) in air-saturated CH_3CN at 20 °C. Inset shows the time course monitored at 570 nm due to the natural decay of **2**.

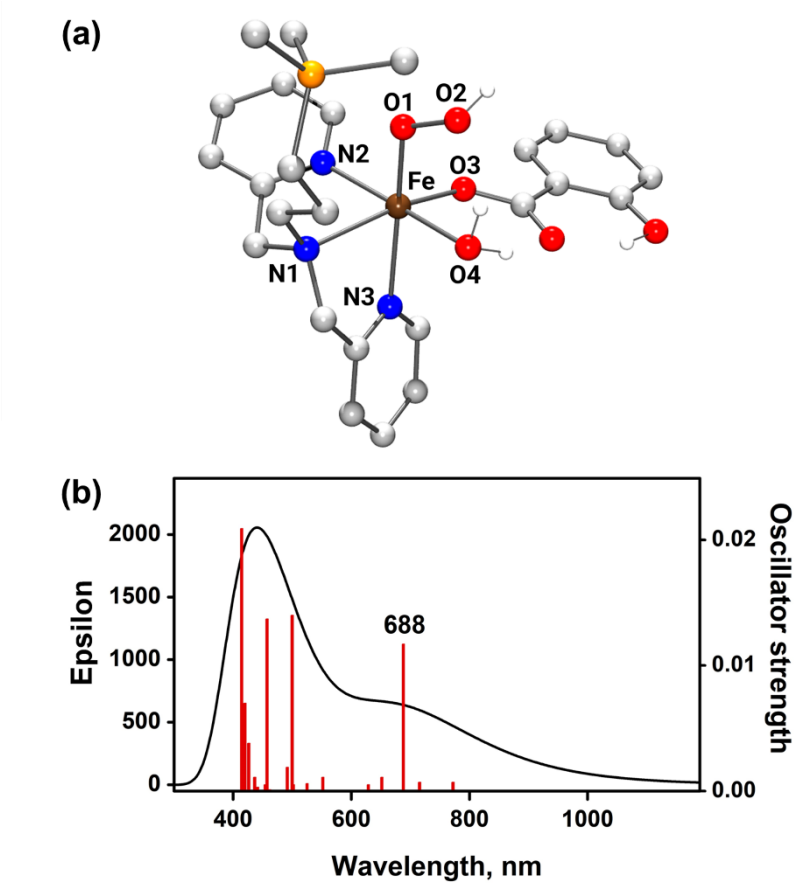

Fig. S4 (a) DFT-optimized structure for **2**. Hydrogens are omitted for clarity except for aqua, salicylate and hydroperoxo ligand. Atom colors: Fe, brown; N, blue; O, red; P, orange; C, grey; H, white**.** (b) simulated UV-vis spectrum according to the optimized structure.

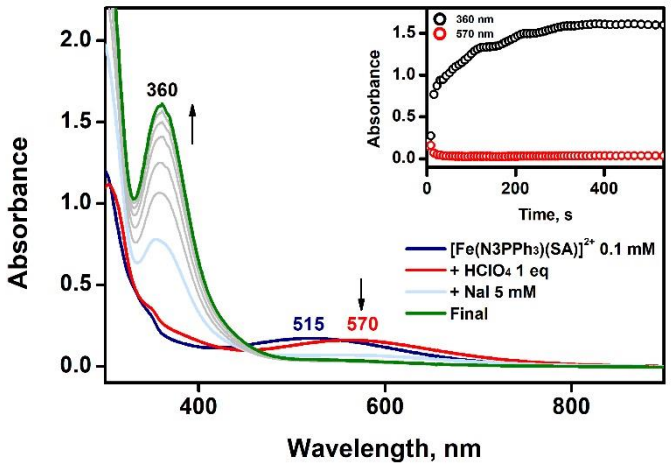

Fig. S5 (a) UV-vis spectral changes obtained in the reaction between **2** (0.50 mM) and NaI (5.0 mM) in CH_3CN at 20 ^oC. Inset shows the time course recorded at 360 nm due to the formation of I_3^-.

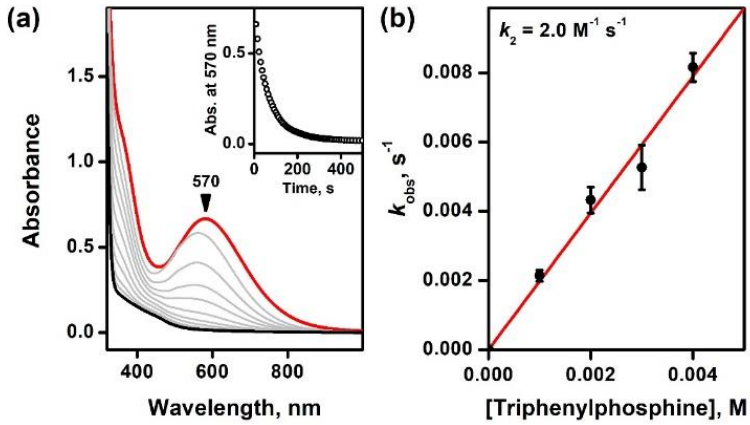

Fig. S6 (a) UV-vis spectral changes obtained in the reaction between **2** (0.50 mM) and triphenylphosphine (5.0 mM) in CH_3CN at 20 °C. (b**)** Plot of k_{obs} against the concentrations of triphenylphosphine obtained in the reaction between **2** (0.50 mM) and substrates in CH_3CN at 20 °C.

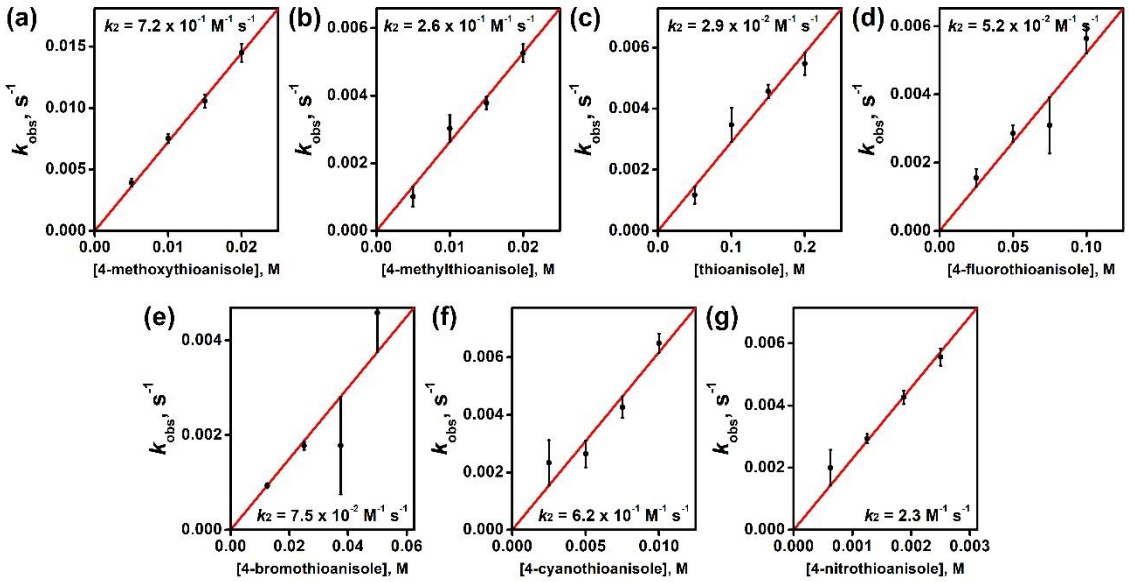

Fig. S7 Plot of k_{obs} against the concentrations of (a) 4-methoxythioanisole, (b) 4-methylthioanisole, (c) thioanisole, (d) 4-fluorothioanisole, (e) 4-bromothioanisole, (f) 4-cyanothioanisole, and (g) 4-nitrothioanisole obtained in the reaction between **2** (0.50 mM) and substrates in CH_3CN at 20 ℃.

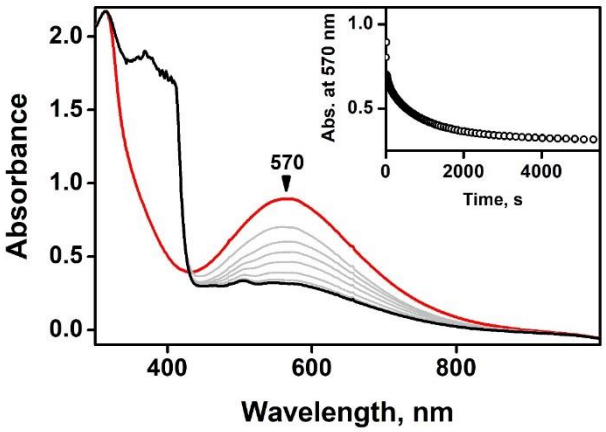

Fig. S8 UV-vis spectral changes obtained in the reaction between **2** (0.50 mM) and 4-nitrothioanisole (25 mM) in CH_3CN at 20 °C.

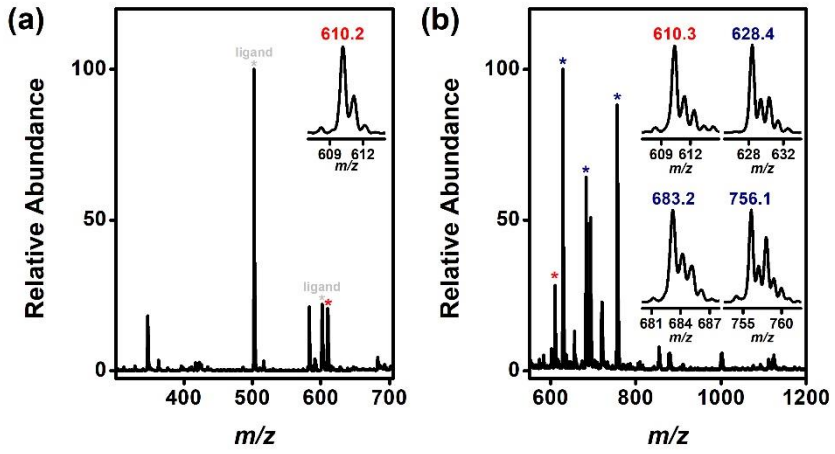

Fig. S9 (a) ESI-MS spectrum of reaction of **2** and thioanisole. The peak at *m/z* = 610.2 corresponds to $[Fe(N3PPh_3)(H_2O)(OH)_2]^+$ (calculated *m/z* = 610.2). (b) ESI-MS spectrum of reaction of **2** and 2,4,6-tri-*tert*-butylphenol. The peaks at *m/z* = 610.3, 628.4, 683.2, and 756.1 correspond to $[Fe(N3PPh_3)(H_2O)(OH)_2]^+$, $[Fe(N3PPh_3)(H_2O)_2(OH)_2]^+$, $[Fe(N3PPh_3)(CH_3CN)(H_2O)_2(OH)(CH_3O)]^+$, and $[Fe(N3PPh_3)(ClO_4)_2]^+$ (calculated *m/z* = 610.2, 628.4, 683.2, and 756.1), respectively.

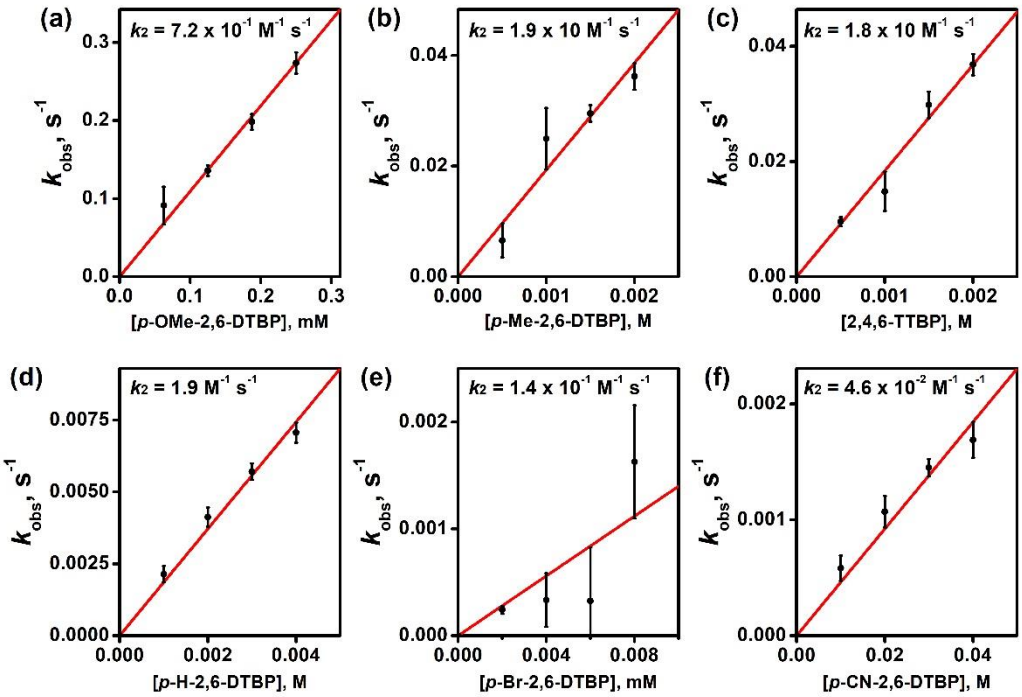

Fig. S10 Plot of k_{obs} against the concentrations of (a) 2,6-di-*tert*-butyl-4-methoxyphenol, (b) 2,6-di-*tert*-butyl-4-methylphenol, (c) 2,4,6-tri-*tert*-butylphenol, (d) 2,6-di-*tert*-butylphenol, (e) 2,6-di-*tert*-butyl-4-bromophenol, and (f) 2,6-di-*tert*-butyl-4-cyanophenol obtained in the reaction between **2** and substrates in CH_3CN at 20 °C.

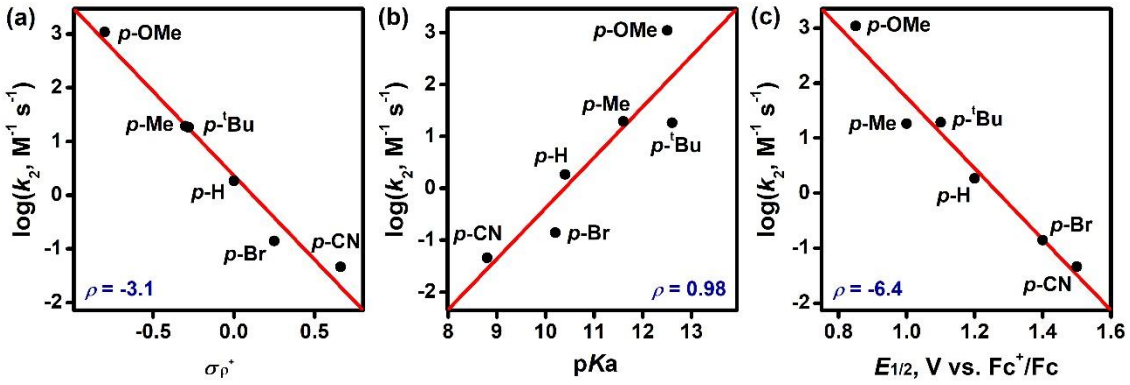

Fig. S11 Plot of log k_2 against (a) σ_p^+, (b) pK_a, and (c) $E_{1/2}$ of 2,6-di-*tert*-butyl-*p*-X-phenol (X = OMe, Me, ^{t}Bu, H, and Br). The $E_{1/2}$ values for *p*-X-2,6-di-*tert*-butylphenol and *p*-CN phenol are not known, hence *p*-X-phenol is used for (c), excluding *p*-CN.

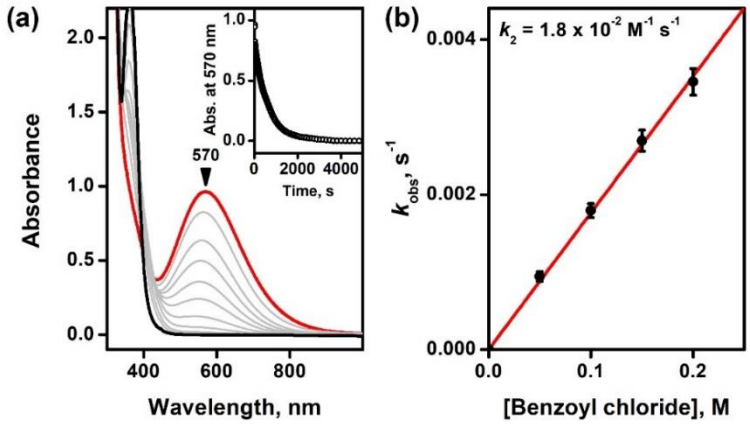

Fig. S12 (a) UV-vis spectral changes obtained in the reaction between **2** (0.50 mM) and benzoyl chloride (100 mM) in CH_3CN at 20 °C. (b) Plot of k_{obs} against the concentrations of benzoyl chloride obtained in the reaction between **2** (0.50 mM) and substrates in CH_3CN at 20 °C.

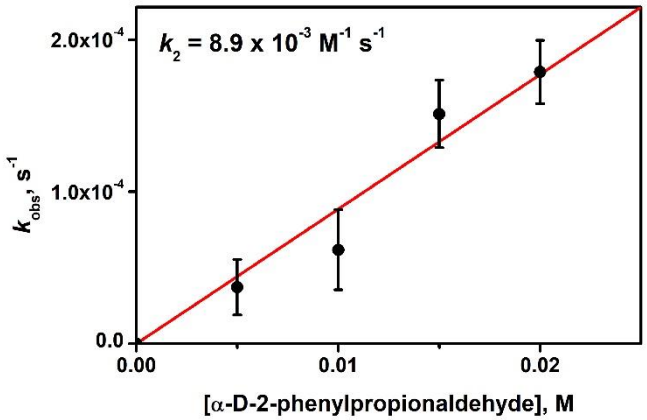

Fig. S13 Plot of k_{obs} against the concentrations of deuterated-2-phenylpropionaldehyde (*d*-2-PPA) obtained in the reaction between **2** (0.10 mM) and *d*-2-PPA in CH_3CN at 20 °C.

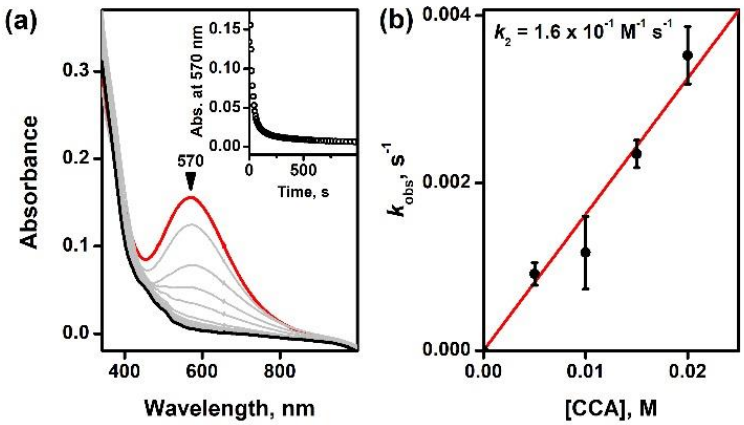

Fig. S14 (a) UV-vis spectral changes obtained in the reaction between **2** (0.10 mM) and cyclohexanecarboxaldehyde (CCA, 10 mM) in CH_3CN at 20 °C. (b) Plot of k_{obs} against the concentrations of CCA obtained in the reaction between **2** (0.10 mM) and CCA in CH_3CN at 20 °C.

.

Coordinates

The coordinates are provided in .xyz-format, with charge/multiplicity in parenthesis in the comment row.

$[Fe(OOH)(N3PPh_3)(SA)(H_2O)]^{2+}$ (**2**)

71

(2/6)

Fe	0.10400	0.22970	-0.04680	H	3.84950	3.85540	-1.20870	H	7.01690	-2.87470	-1.02790
P	-4.99340	-1.93000	-0.49750	H	2.25840	5.40990	-2.37930	H	7.41040	-2.82380	1.42550
N	-1.61700	1.72560	-0.16320	H	-0.17410	4.82780	-2.42890	H	5.67680	-1.89160	2.95650
N	0.98630	2.14610	-0.75530	H	0.93410	-0.86570	2.71080	C	2.80850	-0.93850	-0.58480
N	-0.22300	0.69290	1.99910	H	0.38050	-0.41620	5.11440	O	1.92020	-0.49690	0.25000
C	0.12140	2.98450	-1.36200	H	-1.17790	1.48130	5.64380	O	2.62640	-0.92610	-1.83790
C	-2.99220	1.13220	-0.18270	H	-2.10040	2.84980	3.76740	O	-0.97780	-1.33610	0.20540
C	-4.24130	-2.00250	1.15270	H	-3.07240	0.53780	0.72990	O	-1.07090	-2.27290	-0.89200
C	-6.77940	-2.23040	-0.36600	H	-3.71770	1.95340	-0.10190	H	-0.49250	-2.99630	-0.59230
C	-4.78220	-0.28990	-1.29060	H	-5.21570	-0.41370	-2.28860	H	-4.68210	-1.24040	1.79920
C	-4.24300	-3.21730	-1.53190	H	-5.44090	0.40370	-0.75570	H	-3.16120	-1.85020	1.07000
C	-1.49130	2.54610	1.08210	H	-0.73550	3.31880	0.91660	H	-4.43530	-2.98980	1.58000
C	-1.05580	1.71880	2.26620	H	-2.43230	3.06340	1.29570	H	-7.23530	-1.46800	0.26950
C	-3.34980	0.28440	-1.40720	H	-3.33890	0.90380	-2.30720	H	-6.94960	-3.21670	0.07170
C	-1.32760	2.55590	-1.36180	H	-2.61980	-0.51150	-1.56060	H	-7.23020	-2.19300	-1.36060
C	0.54720	4.17030	-1.95640	H	-1.50980	1.94670	-2.25000	H	-4.65710	-3.17120	-2.54150
C	0.27550	-0.05530	3.00180	H	-1.98830	3.42980	-1.41040	H	-4.46270	-4.19460	-1.09530
C	2.29140	2.46880	-0.70150	C	4.31740	-1.43270	1.35580	H	-3.16080	-3.07130	-1.56110
C	-0.03920	0.20160	4.32940	C	4.07610	-1.45550	-0.03190	O	4.91960	-2.03360	-2.23400
C	-1.42310	2.02540	3.57460	C	5.07170	-1.98230	-0.89740	H	4.03420	-1.63720	-2.42820
C	1.90330	4.49260	-1.92140	C	6.26880	-2.47440	-0.35150	O	0.12910	-0.24870	-2.09820
C	2.79110	3.63220	-1.27480	C	6.47810	-2.44060	1.02070	H	-0.31010	-1.12790	-2.09150
C	-0.90490	1.25890	4.61760	C	5.50350	-1.91700	1.88590	H	1.10890	-0.45470	-2.20960
H	2.93460	1.77370	-0.17550	H	3.55130	-1.02010	2.00260				

References

[S1] W. L. F. Armarego and C. L. L. Chai, *Purification of Laboratory Chemicals,* Butterworth-Heinemann, 6th edn., 2009.

[S2] S. I. Kirin, C. M. Happel, S. Htubanova, T. Weyhermüller, C. Klein and N. Metzler-Nolte, *Dalton Trans.*, 2004, **8**, 1201-1207.

[S3] Gaussian 09, Revision A.02, M.J. Frisch, G.W. Trucks, H.B. Schlegel, G.E. Scuseria, M.A. Robb, J.R. Cheeseman, G. Scalmani, V. Barone, G.A. Petersson, H. Nakatsuji, X. Li, M. Caricato, A. Marenich, J. Bloino, B.G. Janesko, R. Gomperts, B. Mennucci, H.P. Hratchian, J.V. Ortiz, A.F. Izmaylov, J.L. Sonnenberg, D. Williams-Young, F. Ding, F. Lipparini, F. Egidi, J. Goings, B. Peng, A. Petrone, T. Henderson, D. Ranasinghe, V.G. Zakrzewski, J. Gao, N. Rega, G. Zheng, W. Liang, M. Hada, M. Ehara, K. Toyota, R. Fukuda, J. Hasegawa, M. Ishida, T. Nakajima, Y. Honda, O. Kitao, H. Nakai, T. Vreven, K. Throssell, J.A. Montgomery, Jr., J.E. Peralta, F. Ogliaro, M. Bearpark, J.J. Heyd, E. Brothers, K.N. Kudin, V.N. Staroverov, T. Keith, R. Kobayashi, J. Normand, K. Raghavachari, A. Rendell, J.C. Burant, S.S. Iyengar, J. Tomasi, M. Cossi, J.M. Millam, M. Klene, C. Adamo, R. Cammi, J.W. Ochterski, R.L. Martin, K. Morokuma, O. Farkas, J.B. Foresman, D.J. Fox, Gaussian, Inc., Wallingford CT, 2016.

[S4] T. H. Dunning Jr and P. J. Hay, *Journal of Modern Physics*, 1977, **2**.

[S5] P. J. Hay and W. R. Wadt, *J. Chem. Phys.*, 1985, **82**, 270−283.

[S6] W. R. Wadt and P. J. Hay, *J. Chem. Phys.*, 1985, **82**, 284−298.

[S7] P. J. Hay and W. R. Wadt, *J. Chem. Phys.*, 1985, **82**, 299−310.

[S8] R. Ditchfield, W. J. Hehre and J. A. Pople, *J. Chem. Phys.*, 1971, **54**, 724−728.

[S9] W. J. Hehre, R. Ditchfield and J. A. Pople, *J. Chem. Phys.*, 1972, **56**, 2257−2261.

[S10] P. C. Hariharan and J. A. Pople, *Theor. Chem. Acc.*, 1973, **28**, 213−222.

[S11] P. C. Hariharan and J. A. Pople, *Mol. Phys.*, 1974, **27**, 209−214.

[S12] M. S. Gordon, *Chem. Phys. Lett.*, 1980, **76**, 163−168.

[S13] M. M. Francl, W. J. Pietro, W. J. Hehre, J. S. Binkley, D. J. DeFrees, J. A. Pople and M. S. Gordon, *J. Chem. Phys.*, 1982, **77**, 3654−3665.

[S14] R. C. Binning Jr and L. A. Curtiss, *J. Comp. Chem.*, 1990, **11**, 1206−1216.

[S15] J. P. Blaudeau, M. P. McGrath, L. A. Curtiss and L. Radom, *J. Chem. Phys.*, 1997, **107**, 5016−5021.

[S16] V. A. Rassolov, J. A. Pople, M. A. Ratner and T. L. Windus, *J. Chem. Phys.*, 1998, **109**, 1223−1229.

[S17] V. A. Rassolov, M. A. Ratner, J. A. Pople, P. C. Redfern and L. A. Curtiss, *J. Comp. Chem.*, 2001, **22**, 976−984.

[S18] M. Cossi, N. Rega, G. Scalmani and V. Barone, *J. Comput. Chem.*, 2003, **24**, 669−681.

[S19] A. D. McLean and G. S. Chandler, *J. Chem. Phys.*, 1980, **72**, 5639−5648.

[S20] K. Raghavachari, J. S. Binkley, R. Seeger and J. A. Pople, *J. Chem. Phys.*, 1980, **72**, 650−654.

[S21] J. P. Blaudeau, M. P. McGrath, L. A. Curtiss and L. Radom, *J. Chem. Phys.*, 1977, **107**, 5016-5021.

[S22] A. J. H. Wachters, *J. Chem. Phys.*, 1970, **52**, 1033-1036.

[S23] P. J. Hay, *J. Chem. Phys.*, 1977, **66**, 4377-4384.

[S24] K. Raghavachari and G. W. Trucks, *J. Chem. Phys.*, 1989, **91**, 1062−1065.

[S25] R. C. Binning Jr and L. A. Curtiss, *J. Comp. Chem.* 1990, **11**, 1206-1216.

[S26] M. P. McGrath and L. Radom, *J. Chem. Phys.*, 1991, **94**, 511-516.

[S27] L. A. Curtiss, M. P. McGrath, J. P. Blaudeau, N. E. Davis, R. C. Binning Jr and L. Radom, *J. Chem. Phys.*, 1995, **103**, 6104-6113.

[S28] T. Clark, J. Chandrasekhar, G. W. Spitznagel and P. Schleyer, *Comp. Chem.*, 1983, **4**, 294-301.